

Poincaré-Steklov integral Equations and Moduli of Pants

Andrei Bogatyrev

Abstract. Various physical and mathematical settings bring us to a boundary value problem for a harmonic function with spectral parameter in the boundary conditions. One of those problems may be reduced to a singular 1D integral equation with spectral parameter. We present a constructive representation for the eigenvalues and eigenfunctions of this integral equation in terms of moduli of explicitly constructed pants, one of the simplest Riemann surfaces with boundary. Essentially the solution of the integral equation is reduced to the solution of three transcendental equations with three unknown numbers, moduli of pants.

Mathematics Subject Classification (2000). Primary 30Fxx; Secondary 14H15, 30C20, 45C05, 33E30.

Keywords. Spectral parameter, Riemann surface, pair of pants, branched complex projective structure, Dessin d'Enfants.

We introduce the new type of constructive *pictorial* representations for the solutions of the following spectral singular Poincaré–Steklov (PS for brevity) integral equation

$$\lambda \text{ V.p. } \int_I \frac{u(t)}{t-x} dt - \text{V.p. } \int_I \frac{u(t) dR(t)}{R(t) - R(x)} = \text{const}, \quad x \in I := (-1, 1), \quad (0.1)$$

where λ is the spectral parameter; $u(t)$ is the unknown function; *const* is independent of x . The functional parameter $R(t)$ of the equation is a smooth *nondegenerate* change of variable on the interval I :

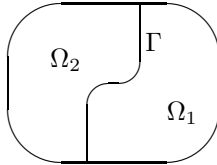
$$\frac{d}{dt}R(t) \neq 0, \quad t \in [-1, 1]. \quad (0.2)$$

1. Introduction

H.Poincaré (1896) and V.A.Steklov (1901) were the first who put the spectral parameter to the boundary conditions of the problem for an elliptic operator. Later it became a popular technique for the analysis and optimization in diffraction problems [1], (thermo)conductivity of composite materials, simple 2D model of oil extraction etc.

1.1. Spectral Boundary Value Problem

Let a domain in the plane be subdivided into two simply connected domains Ω_1 and Ω_2 by a smooth simple arc Γ . We are looking for the values of the spectral parameter λ when the following problem has a nonzero solution:



$$\begin{aligned} \Delta U_1 &= 0 & \text{in } \Omega_1; & \quad U_1 = 0 \text{ on } \partial\Omega_1 \setminus \Gamma; \\ \Delta U_2 &= 0 & \text{in } \Omega_2; & \quad U_2 = 0 \text{ on } \partial\Omega_2 \setminus \Gamma; \\ U_1 &= U_2 & \text{on } \Gamma; & \\ -\lambda \frac{\partial U_1}{\partial n} &= \frac{\partial U_2}{\partial n} & \text{on } \Gamma, & \end{aligned} \quad (1.1)$$

Spectral problems of this type naturally arise e.g. in the justification and optimization of a *domain decomposition method* for the solution of a boundary value problem for Laplace equation. It is easy to show that the eigenfunctions and the eigenvalues of the problem (1.1) are correspondingly the critical points and critical values of the functional (the so called generalized Rayleigh ratio)

$$F(U) = \frac{\int_{\Omega_2} |\text{grad } U_2|^2 d\Omega_2}{\int_{\Omega_1} |\text{grad } U_1|^2 d\Omega_1}, \quad U \in H_{oo}^{1/2}(\Gamma), \quad (1.2)$$

where U_s is the harmonic continuation of the function U from the interface Γ to the domain Ω_s , $s = 1, 2$, vanishing at the outer boundary of the domain.

The boundary value problem (1.1) is equivalent to a certain Poincaré–Steklov equation. Indeed, let V_s be the harmonic function conjugate to U_s , $s = 1, 2$. From the Cauchy–Riemann equations and the relations on Γ it follows that the tangent to the interface derivatives of V_1 and V_2 differ by the same factor $-\lambda$. Integrating along Γ we get

$$\lambda V_1(y) + V_2(y) = \text{const}, \quad y \in \Gamma. \quad (1.3)$$

The boundary values of conjugate functions harmonic in the half-plane are related by a Hilbert transformation. To reduce our case to this model we consider a conformal mapping $\omega_s(y)$ from Ω_s to the open upper half-plane \mathbb{H} with normalization $\omega_s(\Gamma) = I$, $s = 1, 2$. Now equation (1.3) may be rewritten as

$$-\frac{\lambda}{\pi} \text{V.p.} \int_I \frac{U_1(\omega_1^{-1}(t))}{t - \omega_1(y)} dt - \frac{1}{\pi} \text{V.p.} \int_I \frac{U_2(\omega_2^{-1}(t'))}{t' - \omega_2(y)} dt' = \text{const}, \quad y \in \Gamma.$$

Introducing the new notation $x := \omega_1(y) \in I$; $R := \omega_2 \circ \omega_1^{-1} : I \rightarrow \Gamma \rightarrow I$; $u(t) := U_1(\omega_1^{-1}(t))$ and the change of variable $t' = R(t)$ in the second integral we arrive at the Poincaré–Steklov equation (0.1). Note that in this context $R(t)$ is the decreasing function on I .

1.2. Some Known Results

The natural way to study integral equations is operator analysis. This discipline allows to obtain for the *smooth nondegenerate* change of variables $R(x)$ the following results [2]:

- The spectrum is discrete; the eigenvalues are positive and converge to $\lambda = 1$.
- $\sum_{\lambda \in S_p} |\lambda - 1|^2 < \infty$ (a constructive estimate in terms of $R(x)$ is given)
- The eigenfunctions $u(x)$ form a basis in the Sobolev space $H_{oo}^{1/2}(I)$.

1.3. Goal and Philosophy of the Research

The approach of complex geometry for the same integral equation gives different types of results. For quadratic $R(x) = x + (2C)^{-1}(x^2 - 1)$, $C > 1$, the eigenpairs were found explicitly [3]:

$$u_n(x) = \sin \left[\frac{n\pi}{K'} \int_1^{(C+x)/(C-1)} (s^2 - 1)^{-1/2} (1 - k^2 s^2)^{-1/2} ds \right],$$

$$\lambda_n = 1 + 1/\cosh 2\pi\tau n, \quad n = 1, 2, \dots,$$

where $\tau = K/K'$ is the ratio of the complete elliptic integrals of modulus $k = (C - 1)/(C + 1)$. Now we are going to give *constructive representations* for the eigenpairs $\{\lambda, u(x)\}$ of the integral equation with $R(x) = R_3(x)$ being a rational function of degree 3. Equation (0.1) itself will be called PS-3 in this case.

The notion of a constructive representation for the solution should be however specified. Usually this means that we restrict the search for the solution to a certain class of functions such as rational, elementary, abelian, quadratures, the Umemura classical functions, etc. The history of mathematics knows many disappointing results when the solution of the prescribed form does not exist. Say, the diagonal of the square is not commensurable with its side, generic algebraic equations cannot be solved in radicals, linear ordinary differential equations usually cannot be solved by quadratures, Painlevé equations cannot be solved by Umemura functions. Nature always forces us to introduce new types of transcendent objects to enlarge the scope of search. The study of new transcendental functions constitutes the progress of mathematics. This research philosophy goes back to H. Poincaré [4]. From the philosophical point of view our goal is to disclose the nature of emerging transcendental functions in the case of PS-3 integral equations.

1.4. Brief Description of the Result

The rational function $R_3(x)$ of degree three is explicitly related to a *pair of pants* in section 2.2. On the other hand, given a spectral parameter λ and two auxiliary real parameters, we explicitly construct in section 2.3 another pair of pants which additionally depend on two integers. When the above two pants are conformally equivalent, λ is the eigenvalue of the integral equation PS-3 with parameter $R_3(x)$. Essentially, this means that to find the spectrum of the given integral equation (0.1) one has to solve three transcendental equations involving three *moduli of pants*.

Whether this representation of the solutions may be considered as constructive or not is a matter of discussion. Our approach to the notion of a constructive representation is utilitarian: the more we learn about the solution from the given representation the more constructive is the latter. At least we are able to obtain valuable features of the solution: to determine the number of zeroes of the eigenfunction $u(t)$, to find the exact locus for the spectra and to show the discrete mechanism of generating the eigenvalues.

2. Description of the Main Result

The shape of the two domains Ω_1 and Ω_2 defines the variable change $R(x)$ only up to a certain two-parametric deformation. One can easily check that the *gauge transformation* $R \rightarrow L_2 \circ R \circ L_1$, where the linear fractional function $L_s(x)$ keeps the segment $[-1, 1]$, does not affect the spectrum of equation (0.1) and induces only the change of the argument for its eigenfunctions: $u(x) \rightarrow u \circ L_1(x)$. For this reason we do not distinguish between two PS equations with their functional parameters $R(x)$ related by the gauge transformation.

The space of equivalence classes of equations PS-3 has real dimension $3 = 7 - 2 - 2$ and several components with different topology of the functional parameter R_3 . In the present paper we study for brevity only one of the components, the choice is specified in section 2.1.1.

2.1. Topology of the Branched Covering

In what follows we consider *rational degree three* functions $R_3(x)$ with *separate real critical values* different from ± 1 . The rational function $R_3(x)$ defines a 3-sheeted branched covering of a Riemann sphere by another Riemann sphere. The Riemann–Hurwitz formula suggests that $R_3(x)$ has four separate branch points a_s , $s = 1, \dots, 4$. This means that every value a_s is covered by a critical (double) point b_s , and an ordinary point c_s .

Every point $y \neq a_s$ of the extended real axis $\hat{\mathbb{R}} := \mathbb{R} \cup \{\infty\}$ belongs to exactly one of two types. For the type (3:0) the pre-image $R_3^{-1}(y)$ consists of three distinct real points. For the type (1:2) the pre-image consists of a real and two complex conjugate points. The type of the point remains locally constant on the extended real axis and changes when we step over the branch point. Let the branch points

a_s be enumerated in the natural cyclic order of $\hat{\mathbb{R}}$ so that the intervals (a_1, a_2) and (a_3, a_4) are filled with the points of the type (1:2). Later we will specify the way to exclude the relabeling $a_1 \leftrightarrow a_3, a_2 \leftrightarrow a_4$ of branch points.

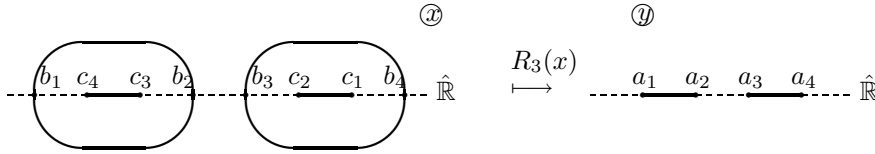


FIGURE 1. The topology of the covering R_3 with real branch points

The total pre-image $R_3^{-1}(\hat{\mathbb{R}})$ consists of the extended real axis and two pairs of complex conjugate arcs intersecting $\hat{\mathbb{R}}$ at the points b_1, b_2, b_3, b_4 as shown at the left side of Fig. 1. The complement of this pre-image on the Riemann sphere has six components, each of them is mapped 1-1 onto the upper or lower half-plane.

2.1.1. The Component in the Space of Equations. The nondegeneracy condition (0.2) forbids that any of critical points b_s be inside the segment of integration $[-1, 1]$. In what follows we consider the case when the latter segment lies in the annulus bounded by two ovals passing through the critical points b_s . Possibly relabeling the branch points we assume that $[-1, 1] \subset (b_2, b_3)$.

Other components in the space of PS-3 integral equations are treated in [11].

2.2. Pair of Pants

For obvious reason a pair of pants is the name for the Riemann sphere with three holes in it. Any pair of pants may be conformally mapped to $\hat{\mathbb{C}} := \mathbb{C} \cup \{\infty\}$ with three nonintersecting real slots. This mapping is unique up to the real linear-fractional transformation of the sphere. The conformal class of pants with labeled boundary components depend on three real parameters varying in a cell.

Definition To the variable change $R_3(x)$ we associate the pair of pants

$$\mathcal{P}(R_3) := \text{Closure} \left(\hat{\mathbb{C}} \setminus \{[-1, 1] \cup [a_1, a_2] \cup [a_3, a_4]\} \right). \tag{2.1}$$

Closure here and below is taken with respect to the intrinsic spherical metrics when every slot acquires two sides. Boundary components of the pair of pants are colored (labeled) in accordance with the palette:

$$\begin{aligned} [-1, 1] & \text{ - "red",} \\ [a_1, a_2] & \text{ - "blue",} \\ [a_3, a_4] & \text{ - "green".} \end{aligned}$$

The conformal class of pants (2.1) depends only on the equivalence class of integral equations. To simplify the statement of our result we assume that infinity lies strictly inside the pants (2.1) which is not a loss of generality – we can always apply a suitable gauge transformation of the parameter $R_3(x)$.

2.2.1. Reconstruction of $R_3(x)$ from the Pants. Here we show that the branched covering map $R_3(x)$ with given branch points a_s , $s = 1, \dots, 4$, is essentially unique. A possible ambiguity is due to the conformal motions of the covering Riemann sphere.

Let L_a be the unique linear-fractional map sending the critical values a_1, a_2, a_3, a_4 of R_3 to respectively $0, 1, a > 1, \infty$. The conformal motion L_b of the covering Riemann sphere sends the critical points b_1, b_2, b_3, b_4 (unknown at the moment) to respectively $0, 1, b > 1, \infty$. The function $L_a \circ R_3 \circ L_b^{-1}$ with normalized critical points and critical values takes a simple form

$$\widetilde{R}_3(x) = x^2 L(x)$$

with a real linear fractional function $L(x)$ satisfying the restrictions:

$$\begin{aligned} L(1) &= 1, & L'(1) &= -2, \\ L(b) &= a/b^2, & L'(b) &= -2a/b^3. \end{aligned}$$

We got four equations for three parameters of $L(x)$ and the unknown b . The first two equations suggest the following expression for $L(x)$

$$L(x) = 1 + 2 \frac{(c-1)(x-1)}{x-c}.$$

Another two are solved parametrically in terms of parameter c :

$$b = c \frac{3c-3}{2c-1}; \quad a = c \frac{(3c-3)^3}{2c-1}.$$

Both functions $b(c)$ and $a(c)$ increase from 1 to ∞ when the argument $c \in (1/3, 1/2)$. So, given $a > 1$ we find the unique c in just specified limits, and therefore the mapping $\widetilde{R}_3(x)$. Now we can restore the linear fractional map L_b . The inverse image \widetilde{R}_3^{-1} of the segment $L_a[-1, 1]$ consists of three disjoint segments. For *our case* we choose the (unique) component of the pre-image belonging to the segment $[1, b]$. The requirement: L_b maps $[-1, 1]$ to the chosen segment determines $R_3(x)$ up to a gauge transformation.

2.3. Another Pair of Pants

For real $\lambda \in (1, 2)$ we consider an annulus α depending on λ bounded by $\varepsilon \widehat{\mathbb{R}}$, $\varepsilon := \exp(2\pi i/3)$, and the circle

$$C := \{p \in \mathbb{C} : |p - \mu^{-1}|^2 = \mu^{-2} - 1\}, \quad \mu := \sqrt{\frac{3-\lambda}{2\lambda}} \in (\frac{1}{2}, 1). \quad (2.2)$$

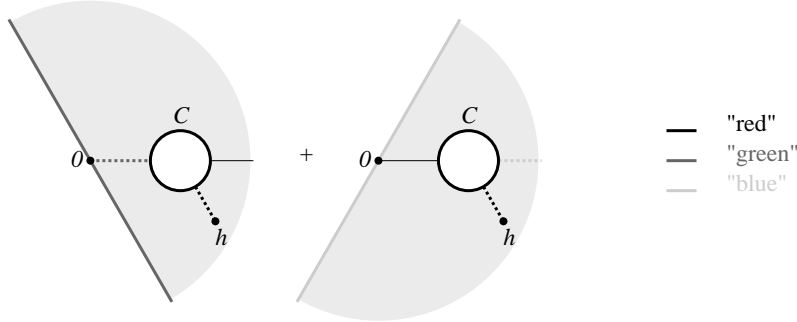
Another annulus bounded by the same circle C and $\varepsilon^2 \widehat{\mathbb{R}}$ is denoted by $\overline{\alpha}$. Note that for the considered values of λ the circle C does not intersect the lines $\varepsilon^{\pm 1} \mathbb{R}$. We paint the boundaries of our annuli in the following way:

$$\begin{aligned} C & \quad - \text{ "red" }, \\ \varepsilon \widehat{\mathbb{R}} & \quad - \text{ "green" }, \\ \varepsilon^2 \widehat{\mathbb{R}} & \quad - \text{ "blue" }. \end{aligned}$$

Given λ in the specified above limits, real h_1, h_2 and nonnegative integers m_1, m_2 , we define three pairs of pants $\mathcal{P}_s(\lambda, h_1, h_2 | m_1, m_2)$ of different fashions $s = 1, 2, 3$.

Fashion 1:

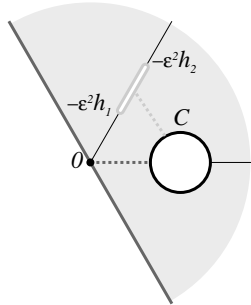
$$\mathcal{P}_1(\lambda, h_1, h_2 | m_1, m_2) := m_1\alpha + m_2\bar{\alpha} +$$



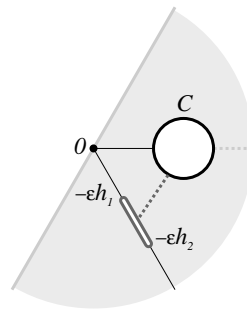
The operations '+' here stand for a certain surgery. First of all take two annuli α and $\bar{\alpha}$ and cut them along the same segment (dashed red line in the figure above) starting at the point $h := h_1 + ih_2$ from the interior of $\alpha \cap \bar{\alpha}$ and ending at the circle C . Now glue the left bank of one cut to the right bank of the other. The resulting two sheeted surface (called *Überlagerungsfläche* in the following) will be the pair of pants $\mathcal{P}_1(\lambda, h_1, h_2 | 0, 0)$. It is possible to modify the obtained surface sewing several annuli to it. Cut the annulus α contained in the pants and m_1 more copies of this annulus along the same segment (shown by the dashed green line in the figure above) connecting the boundaries of the annulus. The left bank of the cut on every copy of α is identified with the right bank of the cut on another copy so that all copies of the annulus are glued in one piece. A similar procedure may be repeated for the annulus $\bar{\alpha}$ (cut along the dashed blue line). The scheme for sewing together fashion 1 pants from the patches $\alpha, \bar{\alpha}$ when $m_1 = 3$ and $m_2 = 2$ is shown in Fig. 2.

Fashions 2 and 3:

$$\mathcal{P}_2(\lambda, h_1, h_2 | m_1, m_2) := m_1\alpha + m_2\bar{\alpha} +$$



$$\mathcal{P}_3(\lambda, h_1, h_2 | m_1, m_2) := m_1\alpha + m_2\bar{\alpha} +$$



The pair of pants $\mathcal{P}_2(\lambda, h_1, h_2|0, 0)$ (resp. $\mathcal{P}_3(\lambda, h_1, h_2|0, 0)$) by definition is the annulus α (resp. $\bar{\alpha}$) with removed segment $-\varepsilon^2[h_1, h_2]$ (resp. $-\varepsilon[h_1, h_2]$), $0 < h_1 < h_2 < \infty$. As in the previous case those pants may be modified by sewing in several annuli $\alpha, \bar{\alpha}$. The scheme of cutting and gluing is shown in Fig. 3

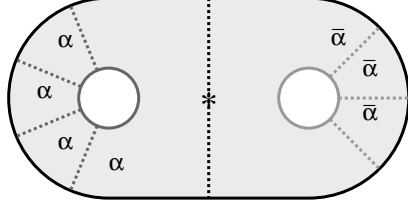


FIGURE 2. The scheme for sewing pants $\mathcal{P}_1(\lambda, h_1, h_2|3, 2)$. Asterisk is the critical point of $p(y)$.

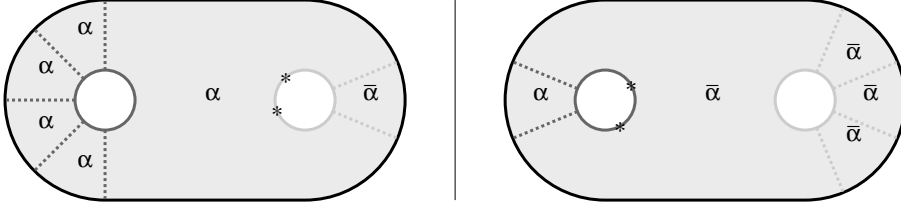


FIGURE 3. The scheme for sewing pants $\mathcal{P}_2(\lambda, h_1, h_2|4, 1)$ (**left**); and $\mathcal{P}_3(\lambda, h_1, h_2|1, 3)$ (**right**). Asterisks are the critical points of the mapping $p(y)$.

2.3.1. Remarks on the Constructed Pairs of Pants. 1. The limiting case of the first fashion of the pants when the branch point $h_1 + ih_2$ tends to $\varepsilon^{\pm 1}\mathbb{R}$ coincides with the limiting cases of the two other fashion pants when $h_1 = h_2 > 0$:

$$\begin{aligned} \mathcal{P}_1(\lambda, -Re(\varepsilon^2 h), -Im(\varepsilon^2 h)|m_1, m_2) &= \mathcal{P}_2(\lambda, h, h|m_1, m_2 + 1), \\ \mathcal{P}_1(\lambda, -Re(\varepsilon h), -Im(\varepsilon h)|m_1, m_2) &= \mathcal{P}_3(\lambda, h, h|m_1 + 1, m_2), \end{aligned} \quad (2.3)$$

where parameter $h > 0$. We denote those intermediate cases as $\mathcal{P}_s(\lambda, h|m_1, m_2)$, $s = 12, 13$ respectively.

2. The surgery procedure of sewing annuli e.g. to the pants (known as *grafting of projective structures*) was designed by B. Maskit (1969), D. Hejhal (1975) and D. Sullivan-W. Thurston (1983), see also W. Goldman (1987).

3. Every pair of pants $\mathcal{P}_s(\lambda, h_1, h_2|m_1, m_2)$ may be conformally mapped to the sphere with three real slots, i.e., pants of the type (2.1). Let $p(y)$ be the inverse mapping. We observe that $p(y)$ has exactly one critical point in the pants $\mathcal{P}(R_3)$, counting *multiplicity and weight*. For the fashion $s = 1$ this point lies strictly inside the pants and is mapped to $h = h_1 + ih_2$. For the case $s = 2$ (resp.

$s = 3$) there will be two simple critical points of $p(y)$ on the blue (resp. green) boundary component of the pants which are mapped to the points $-\varepsilon^2 h_1, -\varepsilon^2 h_2$ (resp. $-\varepsilon h_1, -\varepsilon h_2$). Finally, for the intermediate case (see remark 1) there will be a double critical point on the boundary. The *multiplicity* of the critical point on the boundary should be calculated with respect to the local parameter of the *double* of pants $\mathcal{P}(R_3)$:

$$M := \{w^2 = (y^2 - 1) \prod_{s=1}^4 (y - a_s)\}, \quad (2.4)$$

e.g., at the endpoint $a = \pm 1, a_1, \dots, a_4$ of the slot this local parameter is $\sqrt{y - a}$. We consider the critical points on the boundary with the *weight* $\frac{1}{2}$.

2.4. Main Theorem

Later we explain that *real* eigenfunctions of the integral equation PS-3 are split with respect to the reflection symmetry into two groups: the *symmetric* and the *antisymmetric*. In the present paper we consider only the second group of solutions.

Theorem 2.1. *When $\lambda \neq 1, 3$ the antisymmetric eigenfunctions $u(x)$ of the PS-3 integral equation with parameter $R_3(x)$ are in one to one correspondence with the pants $\mathcal{P}_s(\lambda, h_1, h_2 | m_1, m_2)$, $s = 1, 2, 3, 12, 13$, which are conformally equivalent to the pair of pants $\mathcal{P}(R_3)$ with colored boundary components.*

Let $p(y)$ be the conformal map from $\mathcal{P}(R_3)$ to $\mathcal{P}_s(\lambda, h_1, h_2 | m_1, m_2)$, then up to proportionality

$$u(x) = \sqrt{\frac{(y - y_1)(y - y_2)}{p'(y^+)p'(y^-)} \frac{p(y^+) - p(y^-)}{w(y)}}, \quad (2.5)$$

where $x \in [-1, 1]$; $y := R_3(x)$, $y^\pm := y \pm i0$. For $s = 1$, $y_1 = \overline{y_2}$ is the critical point of the function $p(y)$; for $s = 2, 3$ the real y_1 and y_2 are critical points of the function $p(y)$.

The proof of this theorem will be given in the remaining two sections of the article.

2.5. Corollaries

The representation (2.5) cannot be called explicit in the usual sense, since it comprises a transcendent function $p(y)$. We show that nevertheless the representation is useful as it allows us to understand the following properties of the solutions.

1. The "antisymmetric" part of the spectrum is always a subset of $[1, 2) \cup \{3\}$.
2. Every $\lambda \in (1, 2)$ is the eigenvalue for infinitely many equations PS-3.

Proof. Any of the constructed pants may be transformed to the standard form: a sphere with three real slots. Normalizing the red slot to be $[-1, 1]$, the end points of the two other slots will give the branch points a_1, \dots, a_4 . We know already how to reconstruct the branched covering $R_3(x)$ from its branch points. \square

3. Eigenfunction $u(x)$ related to the pants $\mathcal{P}_s(\dots|m_1, m_2)$ has exactly $m_1 + m_2 + 2$ zeroes on the segment $[-1, 1]$ when $s = 2, 3$ and one more zero when $s = 1$.

Proof. According to the formula (2.5), the number of zeroes of eigenfunction $u(x)$ is equal to the number of points $y \in [-1, 1]$ where $p(y^+) = p(y^-)$. This number in turn is equal to the number of solutions of the inclusion

$$S(y) := \text{Arg}[p(y^-) - \mu^{-1}] - \text{Arg}[p(y^+) - \mu^{-1}] \in 2\pi\mathbb{Z}, \quad y \in [-1, 1]. \quad (2.6)$$

Let the point $p(y)$ go m times around the circle C when its argument y travels along the two sides of $[-1, 1]$. The integer m is naturally related to the integer parameters of the pants $\mathcal{P}_s(\dots)$. The function $S(y)$ strictly increases from 0 to $2\pi m$ on the segment $[-1, 1]$, therefore the inclusion (2.6) has exactly $m + 1$ solutions on the mentioned segment. \square

4. The mechanism for generating the discrete spectrum of the integral equation is explained. Sewing an annulus to the pants $\mathcal{P}_s(\lambda, h_1, h_2|\dots)$ changes the conformal structure of the latter. To return to the conformal structure specified by $\mathcal{P}(R_3)$ we have to change the real parameters of the pants, one of them being the spectral parameter λ .

If we knew how to evaluate the conformal moduli of the pair of pants $\mathcal{P}_s(\lambda, h_1, h_2|m_1, m_2)$ as functions of its real parameters, the solution of the integral equation would be reduced to a system of three transcendental equations for the three numbers λ, h_1, h_2 . This solution will depend on the integer parameters s, m_1, m_2 .

3. Geometry of Integral Equation

PS integral equations possess a rich geometrical structure which we disclose in this section. The chain of equivalent transformations of PS-3 equation described here in a somewhat sketchy fashion is given in [10, 11] with more details.

3.1. A nonlocal Functional Equation

Let us decompose the kernel of the second integral in (0.1) into a sum of elementary fractions:

$$\frac{R'_3(t)}{R_3(t) - R_3(x)} = \frac{d}{dt} \log(R_3(t) - R_3(x)) = \sum_{k=1}^3 \frac{1}{t - x_k(x)} - \frac{Q'}{Q}(t), \quad (3.1)$$

where $Q(t)$ is the denominator in an irreducible representation of $R(t)$ as the ratio of two polynomials; $x_1(x) = x$, $x_2(x)$, $x_3(x)$ – are all solutions (including multiple and infinite) of the algebraic equation $R_3(x_s) = R_3(x)$. This expansion suggests

to rewrite the original equation (0.1) as a certain relationship for the Cauchy-type integral

$$\Phi(x) := \int_I \frac{u(t)}{t-x} dt + \text{const}^*, \quad x \in \hat{\mathbb{C}} \setminus [-1, 1]. \quad (3.2)$$

The constant term const^* in (3.2) is introduced to compensate for the constant terms arising after substitution of expression (3.2) to the equation (0.1).

For a known $\Phi(x)$, the eigenfunction $u(t)$ may be recovered by the Sokhotskii-Plemelj formula:

$$u(t) = (2\pi i)^{-1} [\Phi(t + i0) - \Phi(t - i0)], \quad t \in I. \quad (3.3)$$

Function $\Phi(x)$ generated by an eigenfunction of PS integral equation satisfies a nonlocal functional equation:

Lemma 3.1. [10] *For $\lambda \neq 1, 3$ the transformations (3.2) and (3.3) imply a 1-1 correspondence between the Hölder eigenfunctions $u(t)$ of the PS-3 integral equation and the nontrivial solutions $\Phi(x)$ of the functional equation which are holomorphic on a sphere with the slot $[-1, 1]$*

$$\Phi(x + i0) + \Phi(x - i0) = \delta \left(\Phi(x_2(x)) + \Phi(x_3(x)) \right), \quad x \in I, \quad (3.4)$$

$$\delta = 2/(\lambda - 1), \quad (3.5)$$

with Hölder boundary values $\Phi(x \pm i0)$.

3.2. The Riemann Monodromy Problem

The lifting $R_3^{-1}(\mathcal{P}(R_3))$ of the pants associated to the integral equation consists of three components \mathcal{O}_s , $s = 1, 2, 3$. We number them in the following way (see Fig. 1): the segment $[-1, 1]$ lies on the boundary of \mathcal{O}_1 ; the segment $[c_4, c_3]$ is on the boundary of \mathcal{O}_2 and the boundary of \mathcal{O}_3 comprises the segment $[c_2, c_1]$.

3.2.1. Let the function $\Phi(x)$ be related to the solution $u(x)$ of the integral equation (0.1) as in (3.2). We consider a 3-vector defined in the pair of pants:

$$W(y) := (W_1, W_2, W_3)^t = (\Phi(x_1), \Phi(x_2), \Phi(x_3))^t, \quad y \in \mathcal{P}(R_3), \quad (3.6)$$

where x_s is the unique solution of the equation $R_3(x_s) = y$ in \mathcal{O}_s . Vector $W(y)$ is holomorphic and bounded in the pants $\mathcal{P}(R_3)$ as all three points x_s , $s = 1, 2, 3$, remain in the holomorphicity domain of the function $\Phi(x)$. We claim that *the boundary values of the vector $W(y)$ are related via constant matrices:*

$$W(y + i0) = \mathbf{D}_* W(y - i0), \quad \text{when } y \in \{\text{slot}_*\}. \quad (3.7)$$

The matrix \mathbf{D}_* assigned to the "green" $[a_3, a_4]$, "blue" $[a_1, a_2]$, and "red" $[-1, 1]$ slot respectively is

$$\mathbf{D}_2 := \left\| \begin{array}{ccc} 0 & 0 & 1 \\ 0 & 1 & 0 \\ 1 & 0 & 0 \end{array} \right\|; \quad \mathbf{D}_3 := \left\| \begin{array}{ccc} 0 & 1 & 0 \\ 1 & 0 & 0 \\ 0 & 0 & 1 \end{array} \right\|; \quad \mathbf{D} := \left\| \begin{array}{ccc} -1 & \delta & \delta \\ 0 & 1 & 0 \\ 0 & 0 & 1 \end{array} \right\|. \quad (3.8)$$

This in particular means that our vector (3.6) is a solution of a certain Riemann monodromy problem. The monodromy of vector $W(y)$ along the loop crossing only "red", "green" or "blue" slot is given by the matrix \mathbf{D} , \mathbf{D}_2 or \mathbf{D}_3 correspondingly – see Fig. 4.

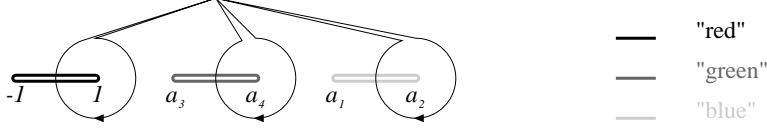


FIGURE 4. Three loops on a sphere with six punctures $\pm 1, a_1, \dots, a_4$

Indeed, let $y^+ := y + i0$ and $y^- := y - i0$ be two points on opposite sides of the "blue" slot $[a_1, a_2]$. Their inverse images $x_3^+ = x_3^-, x_1^\pm = x_2^\mp$ lie outside the cut $[-1, 1]$. Hence $W(y^+) = \mathbf{D}_3 W(y^-)$. For two points y^\pm lying on opposite sides of the "green" slot $[a_3, a_4]$, their inverse images satisfy relations $x_2^+ = x_2^-, x_1^\pm = x_3^\mp$, which means $W(y^+) = \mathbf{D}_2 W(y^-)$. Finally, let y^\pm lie on both sides of the "red" slot $[-1, 1]$. Now two points $x_2^+ = x_2^-$ and $x_3^+ = x_3^-$ lie in the holomorphicity domain of $\Phi(x)$ while x_1^+ and x_1^- appear on the opposite sides of the cut $[-1, 1]$. According to the functional equation (3.4),

$$\Phi(x_1^+) = -\Phi(x_1^-) + \delta(\Phi(x_2^\pm) + \Phi(x_3^\pm)),$$

therefore $W(y^+) = \mathbf{D}W(y^-)$ holds on the slot $[-1, 1]$.

3.2.2. Conversely, let $W(y)$ be the bounded solution of the Riemann monodromy problem (3.7). We define a piecewise holomorphic function on the Riemann sphere:

$$\Phi(x) := W_s(R_3(x)), \quad \text{when } x \in \mathcal{O}_s, \quad s = 1, 2, 3. \quad (3.9)$$

From the boundary relations for the vector $W(y)$ it immediately follows that the function $\Phi(x)$ has no jumps on the lifted cuts $[a_1, a_2]$, $[a_3, a_4]$, $[-1, 1]$ except for the cut $[-1, 1]$ from the upper sphere. Say, if the two points y^\pm lie on opposite sides of the cut $[a_1, a_2]$, then $W_3(y^+) = W_3(y^-)$ and $W_1(y^\pm) = W_2(y^\mp)$ which means that the function $\Phi(x)$ has no jump on the components of $R_3^{-1}[a_1, a_2]$. From the boundary relation on the cut $[-1, 1]$ it follows that $\Phi(x)$ is the solution for the functional equation (3.4). Therefore it gives a solution of Poincaré–Steklov integral equation with parameter $R_3(x)$. Combining formulae (3.3) with (3.9) we get the reconstruction rule

$$u(x) = (2\pi i)^{-1} \left(W_1(R_3(x) + i0) - W_1(R_3(x) - i0) \right), \quad x \in [-1, 1]. \quad (3.10)$$

We have just proved the following

Theorem 3.2. [3] *If $\lambda \neq 1, 3$ then the two formulas (3.6) and (3.10) imply the one-to-one correspondence between the solutions $u(x)$ of the integral equation (0.1) and the bounded solutions $W(y)$ of the Riemann monodromy problem (3.7) in the punctured sphere $\hat{\mathbb{C}} \setminus \{-1, 1, a_1, a_2, a_3, a_4\}$.*

3.2.3. Monodromy Invariant. The following statement is proved by direct computation.

Lemma 3.3. *All matrixes (3.8) (i) are involutive (i.e. $\mathbf{D}^2 = \mathbf{D}_2^2 = \mathbf{D}_3^2 = \mathbf{1}$) and (ii) conserve the quadratic form*

$$J(W) := \sum_{k=1}^3 W_k^2 - \delta \sum_{j<s}^3 W_j W_s. \quad (3.11)$$

The form $J(W)$ is not degenerate unless $-2 \neq \delta \neq 1$, or equivalently $0 \neq \lambda \neq 3$. Since the solution $W(y)$ of our monodromy problem is bounded near the cuts, the value of the form $J(W)$ is independent of the variable y . Therefore the solution takes values either in the smooth quadric $\{W \in \mathbb{C}^3 : J(W) = J_0 \neq 0\}$, or the cone $\{W \in \mathbb{C}^3 : J(W) = 0\}$.

3.3. Geometry of the Quadric Surface

The nondegenerate projective quadric $\{J(W) = J_0\}$ contains two families of line elements¹ which for convenience are denoted by the signs '+' and '-'. Two different lines from the same family are disjoint while two lines from different families must intersect. The intersection of those lines with the 'infinitely distant' secant plane gives points on the conic

$$\mathcal{C} := \{(W_1 : W_2 : W_3)^t \in \mathbb{C}P^2 : J(W) = 0\} \quad (3.12)$$

which by means of the stereographic projection p may be identified with the Riemann sphere. Therefore we have introduced two global coordinates $p^\pm(W)$ on the quadric, the 'infinite part' of which (= conic \mathcal{C}) corresponds to coinciding coordinates: $p^+ = p^-$ (see fig. 5).

The natural action of them pseudo-orthogonal group $O_3(J)$ in \mathbb{C}^3 conserves the quadric, the conic at infinity \mathcal{C} , and the families of line elements possibly interchanging their labels ' \pm '. The induced action of the group $O_3(J)$ on the stereographic coordinates p^\pm is a linear fractional with a possible change of the superscript ' \pm '.

3.3.1. Stereographic Coordinates. To obtain explicit expressions for the coordinate change $W \leftrightarrow p^\pm$ on the quadric we bring the quadratic form $J(W)$ to the simpler form $J_\bullet(V) := V_1 V_3 - V_2^2$ by means of the linear coordinate change

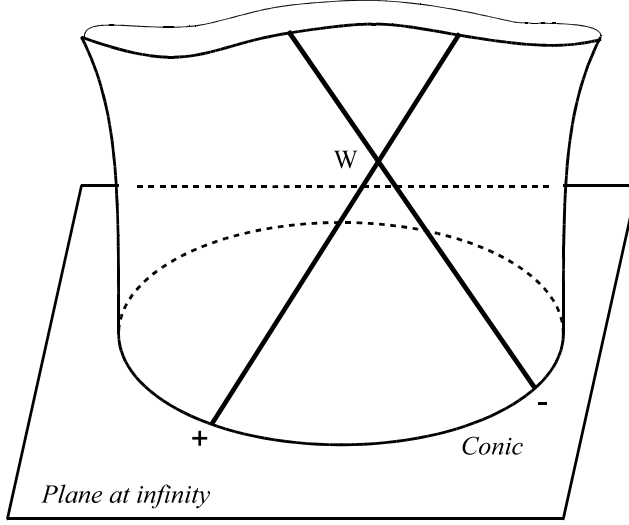
$$W = \mathbf{K}V \quad (3.13)$$

where

$$\mathbf{K} := (3\delta + 6)^{-1/2} \begin{pmatrix} 1 & 1 & 1 \\ 1 & \varepsilon^2 & \varepsilon \\ 1 & \varepsilon & \varepsilon^2 \end{pmatrix} \cdot \begin{pmatrix} 0 & \mu^{-1} & 0 \\ 0 & 0 & 1 \\ 1 & 0 & 0 \end{pmatrix}, \quad (3.14)$$

$$\varepsilon := \exp(2\pi i/3), \quad \mu := \sqrt{\frac{\delta-1}{\delta+2}} = \sqrt{\frac{3-\lambda}{2\lambda}}.$$

¹This property of quadric is sometimes used in architecture. The line generators of the hyperboloid serve as construction elements, e.g., for the Shukhov tower in Moscow.

FIGURE 5. Global coordinates p^+ and p^- on quadric

Translating the first paragraph of the current section into formulae we get

$$p^\pm(W) := \frac{V_2 \pm i\sqrt{J_0}}{V_1} = \frac{V_3}{V_2 \mp i\sqrt{J_0}}; \quad (3.15)$$

and inverting this dependence,

$$W(p^+, p^-) = \frac{2i\sqrt{J_0}}{p^+ - p^-} \mathbf{K} \begin{pmatrix} 1 \\ (p^+ + p^-)/2 \\ p^+ p^- \end{pmatrix}. \quad (3.16)$$

The point $W(p^+, p^-)$ with coordinate p^+ (resp. p^-) being fixed moves on the straight line with the directing vector $\mathbf{K}(1 : p^+ : (p^+)^2)$ (resp. $\mathbf{K}(1 : p^- : (p^-)^2)$) belonging to the conic (3.12).

3.3.2. Action of the Pseudo-orthogonal Group.

Lemma 3.4. *There exists a (spinor) representation $\chi : O_3(J) \rightarrow PSL_2(\mathbb{C})$ such that:*

- 1) *The restriction of $\chi(\cdot)$ to $SO_3(J)$ is an isomorphism to $PSL_2(\mathbb{C})$.*
- 2) *For coordinates p^\pm on the quadric the following transformation rule holds:*

$$\begin{aligned} p^\pm(\mathbf{T}W) &= \chi(\mathbf{T})p^\pm(W), & \mathbf{T} &\in SO_3(J), \\ p^\pm(\mathbf{T}W) &= \chi(\mathbf{T})p^\mp(W), & \mathbf{T} &\notin SO_3(J). \end{aligned} \quad (3.17)$$

3) The linear-fractional mapping $\chi p := (ap+b)/(cp+d)$ is the image of the matrix:

$$\mathbf{T} := \frac{1}{ad-bc} \mathbf{K} \begin{vmatrix} d^2 & 2cd & c^2 \\ bd & ad+bc & ac \\ b^2 & 2ab & a^2 \end{vmatrix} \mathbf{K}^{-1} \in SO_3(J). \quad (3.18)$$

4) The generators of the monodromy group are mapped to the following elements of PSL_2 :

$$\begin{aligned} \chi(\mathbf{D}_s)p &= \varepsilon^{1-s}/p, & s &= 1, 2, 3; \\ \chi(\mathbf{D})p &= \frac{\mu p - 1}{p - \mu}. \end{aligned} \quad (3.19)$$

Proof. We define the action of the matrix $\mathbf{A} \in SL_2(\mathbb{C})$ on the vector $V \in \mathbb{C}^3$ by the formula:

$$\mathbf{A} := \begin{vmatrix} a & b \\ c & d \end{vmatrix}; \quad \begin{vmatrix} V_3 & V_2 \\ V_2 & V_1 \end{vmatrix} \longrightarrow \mathbf{A} \begin{vmatrix} V_3 & V_2 \\ V_2 & V_1 \end{vmatrix} \mathbf{A}^t. \quad (3.20)$$

It is easy to check that (3.20) gives the faithful representation of a connected 3-dimensional group $PSL_2(\mathbb{C}) := SL_2(\mathbb{C})/\{\pm 1\}$ into $SO_3(J_\bullet)$ and therefore, an isomorphism. Let us denote by χ_\bullet the inverse isomorphism $SO_3(J_\bullet) \rightarrow PSL_2(\mathbb{C})$ and let $\chi(\pm \mathbf{T}) := \chi_\bullet(\mathbf{K}^{-1} \mathbf{T} \mathbf{K})$ for $\mathbf{T} \in SO_3(J)$. The obtained homomorphism $\chi : O_3(J) \rightarrow PSL_2(\mathbb{C})$ will satisfy statement 1) of the lemma.

To prove 2) we replace components of the vector V in the right-hand side of (3.20) with their representation in terms of the stereographic coordinates p^\pm :

$$\begin{aligned} & \frac{i\sqrt{J_0}}{p^+ - p^-} \mathbf{A} [(p^+, 1)^t \cdot (p^-, 1) + (p^-, 1)^t \cdot (p^+, 1)] \mathbf{A}^t = \\ & i\sqrt{J_0} \frac{(cp^+ + d)(cp^- + d)}{p^+ - p^-} [(\chi p^+, 1)^t \cdot (\chi p^-, 1) + (\chi p^-, 1)^t \cdot (\chi p^+, 1)] = \\ & \frac{i\sqrt{J_0}}{\chi p^+ - \chi p^-} [(\chi p^+, 1)^t \cdot (\chi p^-, 1) + (\chi p^-, 1)^t \cdot (\chi p^+, 1)] = \\ & \quad \begin{vmatrix} V_3(\chi p^+, \chi p^-) & V_2(\chi p^+, \chi p^-) \\ V_2(\chi p^+, \chi p^-) & V_1(\chi p^+, \chi p^-) \end{vmatrix}, \end{aligned}$$

where we set $\chi p := (ap+b)/(cp+d)$. Now (3.17) follows immediately for $\mathbf{T} \in SO_3(J)$. It remains to check the transformation rule for any matrix \mathbf{T} from the other component of the group $O_3(J)$, say $\mathbf{T} = -\mathbf{1}$.

Writing the action (3.20) component-wise we arrive at conclusion 3) of the lemma.

And finally, expressions 4) for the generators of monodromy group may be obtained either from analyzing formula (3.18) or from finding the eigenvectors of the matrices \mathbf{D}_s, \mathbf{D} which correspond to the fixed points of linear-fractional transformations. \square

For convenience we collect all the introduced objects related to the boundary components of the pair of pants $\mathcal{P}(R_3)$ in Tab. 1

TABLE 1. Slots, their associated colors, matrices and linear-fractional maps

slot	$[-1, 1]$	$[a_1, a_2]$	$[a_3, a_4]$
color	"red"	"blue"	"green"
matrix \mathbf{D}_*	$\mathbf{D} := \begin{vmatrix} -1 & \delta & \delta \\ 0 & 1 & 0 \\ 0 & 0 & 1 \end{vmatrix}$	$\mathbf{D}_3 := \begin{vmatrix} 0 & 1 & 0 \\ 1 & 0 & 0 \\ 0 & 0 & 1 \end{vmatrix}$	$\mathbf{D}_2 := \begin{vmatrix} 0 & 0 & 1 \\ 0 & 1 & 0 \\ 1 & 0 & 0 \end{vmatrix}$
$\chi(\mathbf{D}_*)p$	$\frac{\mu p - 1}{p - \mu}$	ε/p	ε^2/p

3.4. Entangled Projective Structures

Definition 3.5. A branched complex projective structure [5, 6, 8, 9] on a Riemann surface \mathcal{M} is a meromorphic function $p(t)$ on the universal covering $\tilde{\mathcal{M}}$ which transforms fractionally linear under the cover transformations of $\tilde{\mathcal{M}}$. The appropriate representation $\chi : \pi_1(\mathcal{M}) \rightarrow PSL_2(\mathbb{C})$ is called the *monodromy* of the projective structure. The set of all critical points of $p(t)$ with their multiplicities survives under the cover transformations of $\tilde{\mathcal{M}}$. The projection of this set to the Riemann surface \mathcal{M} is known as the *branching divisor* $D(p)$ of projective structure and the branching number of the structure $p(t)$ is $\deg D(p)$.

Examples. The unbranched projective structures arise in Fuchsian and Schottky uniformizations of the Riemann surface. Any meromorphic function on a Riemann surface is a branched projective structure with trivial monodromy.

3.4.1. Projective Structures Generated by Eigenfunction. Every bounded solution $W(y)$ of the Riemann monodromy problem (3.7) generates two nowhere coinciding meromorphic functions $p^\pm(y)$ in the sphere with three slots. Those functions are stereographic coordinates (3.15) for the vector $W(y)$. The boundary values of functions $p^+(y)$ and $p^-(y)$ on every slot are related by linear-fractional transformations:

$$p^\pm(y + i0) = \chi(\mathbf{D}_*)p^\mp(y - i0), \quad y \in \{slot_*\} \quad (3.21)$$

where the matrix $\mathbf{D}_* = \mathbf{D}, \mathbf{D}_2, \mathbf{D}_3$ stand for the 'red', 'green' and 'blue' slots respectively.

Relations (3.21) allow us to analytically continue both functions $p^+(y)$ and $p^-(y)$ through any slot to the second sheet of the genus 2 Riemann surface

$$M := \{w^2 = (y^2 - 1) \prod_{s=1}^4 (y - a_s)\}, \quad (3.22)$$

and further to its universal covering \tilde{M} . Thus obtained functions $p^\pm(t), t \in \tilde{M}$, will be locally single valued on the Riemann surface since all matrices \mathbf{D}_* are involutive. However varying the argument t along the handle of the surface M may result in a linear-fractional transformation of the value $p^\pm(t)$. Say, the continuations of $p^+(y)$

from the pants through the red and green slots will give two different functions on the second sheet related by the linear-fractional mapping $\chi(\mathbf{DD}_2)$.

3.4.2. Branching of the Structures p^\pm . The way we have carried out the continuation of functions $p^\pm(y)$ suggests that the branching divisors of the arising projective structures are related via the hyperelliptic involution $H(y, w) := (y, -w)$ of the surface M :

$$D(p^+) = HD(p^-). \quad (3.23)$$

The condition $p^+ \neq p^-$ allows to determine the branching numbers of the structures which is done in the next theorem.

Theorem 3.6. [11] *When $\lambda \notin \{0, 1, 3\}$ the solutions $u(x)$ of the integral equation PS-3 that have invariant $J_0 \neq 0$ are in one-to-one correspondence with the couples of not identically equal functions meromorphic in the pants $\mathcal{P}(R_3)$ $p^\pm(y)$ with boundary values satisfying (3.21) and two critical points in common. The correspondence $u(x) \rightarrow p^\pm(y)$ is established by the sequence of formulae (3.2), (3.6) and (3.15); the inverse dependence is given by the formula*

$$2\pi u(x) = \sqrt{\frac{(\delta + 2)J_0}{3} \frac{p^+(y)p^-(y) - \mu(p^+(y) + p^-(y)) + 1}{p^+(y) - p^-(y)}}, \quad (3.24)$$

where $x \in [-1, 1]$ and $y := R_3(x) + i0$.

Remark: The number of critical points of the structures in the pants is counted with their *weight and multiplicity* (see remark 3 on page 8): 1) the branching number of $p^\pm(y)$ at the branch point $a \in \{\pm 1, a_1, \dots, a_4\}$ of M is computed with respect to the local parameter $z = \sqrt{y - a}$, 2) every branch point of the projective structure on the boundary of the pants should be considered as a half-point.

Proof. : 1. Let $u(x)$ be an eigenfunction of the integral equation PS-3, then the stereographic coordinates $p^\pm(y)$ of the solution of the associated Riemann monodromy problem inherit the boundary relationship (3.21). What remains is to find the branching numbers of the entangled structures $p^\pm(y)$. To this end we consider the *Kleinian quadratic differential* on the slit sphere

$$\Omega(y) = \frac{dp^+(y)dp^-(y)}{(p^+(y) - p^-(y))^2}, \quad y \in \hat{\mathbb{C}}. \quad (3.25)$$

This expression is the infinitesimal form of the cross ratio, hence it remains unchanged after the same linear-fractional transformations of the functions p^+ and p^- . Therefore, (3.25) is a well defined quadratic differential on the entire sphere. Lifting $\Omega(y)$ to the surface M we get a holomorphic differential. Indeed, $p^+ \neq p^-$ everywhere and applying suitable linear-fractional transformation we assume that $p^+ = 1 + z^{m_+} + \{\text{terms of higher order}\}$ and $p^- = cz^{m_-} + \dots$ in terms of local parameter z of the surface, $m_\pm \geq 1$, $c \neq 0$. Then $\Omega = cm_+m_-z^{m_++m_- - 2} + \{\text{terms of higher order}\}$. Therefore

$$D(p^+) + D(p^-) = (\Omega).$$

Any holomorphic quadratic differential on a genus 2 surface has 4 zeroes and taking into account the symmetry (3.23) of the branching divisors, we see that each of the structures p^\pm has the branching number two on the curve M . It remains to note that the pair of pants $\mathcal{P}(R_3)$ are exactly "one half" of M .

2. Conversely, let $p^+(y)$ and $p^-(y)$ be two not identically equal meromorphic functions on the slit sphere, with boundary conditions (3.21) and total branching number two in the pants (see remark above). We can prove that $p^+ \neq p^-$ everywhere. Indeed, for the meromorphic quadratic differential (3.25) on the Riemann surface M we establish (using a local coordinate on the surface) the inequality

$$D(p^+) + D(p^-) \geq (\Omega) \quad (3.26)$$

where the deviation from equality means that there is a point where $p^+ = p^-$. But the degree of the divisor on the left of (3.26) is four and the same number is $\deg(\Omega) = 4g - 4$. Therefore this pair of functions p^\pm will give us the holomorphic vector $W(p^+(y), p^-(y))$ in the pants which solves our Riemann monodromy problem. We already know how to convert the latter vector to the eigenfunction of the integral equation PS-3. \square

3.4.3. Remark about the Non-smooth Quadric. It is shown in [11] how to incorporate the exceptional case $J_0 = 0$ into the above scheme. In the latter case the functions $p^\pm(y)$ coincide, however the boundary relations (3.21) survive. The total branching number of the function $p^+ = p^-$ in the pair of pants is either zero or one. The solutions to the PS-3 integral equation and the associated Riemann monodromy problem may be recovered up to proportionality from the unified formulae (true whatever J_0)

$$u(x) = \sqrt{\frac{\Omega(y)}{dp^+(y)dp^-(y)}}(p^+(y)p^-(y) - \mu(p^+(y) + p^-(y)) + 1), \quad (3.27)$$

$$W(y) = \sqrt{\frac{\Omega(y)}{dp^+(y)dp^-(y)}}\mathbf{K}(1, (p^+(y) + p^-(y))/2, p^+(y)p^-(y))^t, \quad (3.28)$$

where $\Omega(y) = (y - y_1)(y - y_2)\frac{(dy)^2}{w^2(y)}$ is the holomorphic quadratic differential on the Riemann surface M with zeroes at the branching points of the possibly coinciding structures p^+ and p^- [or with two arbitrary double zeroes when the structure $p^+ = p^-$ is unbranched, further analysis however shows that the required unbranched structures do not exist].

3.5. Types of the Mirror Symmetry of the Solution

The eigenvalues of the integral equation are the critical values of the *positive* functional (1.2) – the generalized Rayleigh ratio. So we may consider only *real* eigenfunctions $u(x)$ without loss of generality. Real solutions of the PS-3 equation

give rise to exactly two types of *mirror symmetry* for the entangled structures:

$$\begin{aligned} \textit{Symmetric} & \quad p^\pm(\bar{y}) = 1/\overline{p^\pm(y)} \\ \textit{Antisymmetric} & \quad p^\pm(\bar{y}) = 1/p^\mp(y) \end{aligned}, \quad y \in \mathcal{P}(R_3),$$

depending on the sign of the real number $(\delta + 2)J_0$. In what follows we restrict ourselves to the case of *antisymmetric eigenfunctions*. In this case:

$$p^+(y \pm i0) = 1/\overline{p^-(y \mp i0)} = 1/\chi(\mathbf{D}_*)p^+(y \pm i0), \quad y \in \textit{slot}_*,$$

and hence we know where the boundary components of the pair of pants $\mathcal{P}(R_3)$ are mapped to. In particular,

$$\begin{aligned} \textit{"green" boundary} & \rightarrow \varepsilon\hat{\mathbb{R}} \\ \textit{"blue" boundary} & \rightarrow \varepsilon^2\hat{\mathbb{R}} \\ \textit{"red" boundary} & \rightarrow \begin{cases} C & - \textit{see (2.2)} \quad \textit{when } 1 < \lambda < 3 \\ \emptyset & \textit{when } \lambda < 1 \textit{ or } 3 < \lambda. \end{cases} \end{aligned} \quad (3.29)$$

We see that the above geometrical analysis of the integral equation gives the universal limits for (the antisymmetric part of) the spectrum.

The branching divisor of the projective structure p^+ has the mirror symmetry: $D(p^+) = \bar{H}D(p^+)$ where $\bar{H}(y, w) := (\bar{y}, -\bar{w})$ is the anticonformal involution of the surface M leaving boundary components (ovals) of pair of the pants $\mathcal{P}(R_3)$ intact. Therefore exactly three situations may occur: $p^+(y)$ has one simple critical point strictly inside the pants, or there are two simple critical points on the boundary of pants or there is one double critical point of $p^+(y)$ on the boundary of the pants.

4. Combinatorics of Integral Equation

For the antisymmetric eigenfunctions we arrive at the essentially combinatorial **Problem** (about putting pants on a sphere) *Find a meromorphic function $p := p^+$ defined in the pair of pants $\mathcal{P}(R_3)$ mapping boundary ovals to the given circles (3.29) and having exactly one critical point (counted with weight and multiplicity) in the pants.*

The three above-mentioned types of the branching divisor $D(p)$ will be treated separately in the sections 4.1, 4.2. When the branch point of the structure p is strictly inside the pants we show that the solution of the problem takes the form of the Überlagerungsfläche $\mathcal{P}_1(\dots)$ with certain real and integer parameters. The case of two simple branch points belonging to the boundary gives us the pants $\mathcal{P}_s(\dots)$, $s = 2, 3$ and the unstable intermediate case with double branch point on the boundary brings us to the pants $\mathcal{P}_j(\dots)$, $j = 12, 13$ described in (2.3).

Let $p(y)$ be a holomorphic map from a Riemann surface \mathcal{M} with a boundary to the sphere and the selected boundary component $(\partial\mathcal{M})_*$ be mapped to a circle. The reflection principle allows us to holomorphically continue $p(y)$ through this selected component to the double of \mathcal{M} . Therefore we can talk of the critical points of $p(y)$ on $(\partial\mathcal{M})_*$. When the argument y passes through a simple critical point, the value $p(y)$ reverses the direction of its movement on the circle. So there should

be an even number of critical points (counted with multiplicities) on the selected boundary component.

4.1. The Branchpoint is inside a Pair of Pants

4.1.1. Construction 1. Using otherwise a composition with a suitable linear-fractional map, we suppose that the circle $p((\partial\mathcal{M})_*)$ is the boundary of the unitary disc

$$\mathbb{U} := \{p \in \mathbb{C} : |p| \leq 1\}, \quad (4.1)$$

and that a small annular vicinity of the selected boundary component is mapped to the exterior of the unit disc. We define the mapping of a disjoint union $\mathcal{M} \cup \mathbb{U}$ to a sphere

$$\tilde{p}(y) := \begin{cases} p(y), & y \in \mathcal{M}, \\ L(y^d), & y \in \mathbb{U}, \end{cases} \quad (4.2)$$

where the integer $d > 0$ is the degree of the mapping $p : (\partial\mathcal{M})_* \rightarrow \partial\mathbb{U}$, and where $L(y)$ is an (at the moment arbitrary) linear fractional mapping keeping the unitary disc (4.1) unchanged. The choice of $L(\cdot)$ will be fixed later to simplify the arising combinatorial analysis.

Now we fill in the hole in \mathcal{M} by the unit disc, identifying the points of $(\partial\mathcal{M})_*$ and the points of $\partial\mathbb{U}$ with the same value of \tilde{p} (there are d ways to do so). The holomorphic mapping $\tilde{p}(y)$ of the new Riemann surface $\mathcal{M} \cup \mathbb{U}$ to the sphere will have exactly one additional critical point of multiplicity $d - 1$ at the center of the glued disc.

4.1.2. Branched Covering of a Sphere. We return to the function $p(y)$ being the solution of the problem stated in the beginning of section 4. Suppose that the point $p(y)$ completes turns on the corresponding circle d_r , d_g and d_b times when the argument y runs around the 'red', 'green' and 'blue' boundary component of $\mathcal{P}(R_3)$ respectively. We can apply the just introduced *construction 1* and glue the three discs \mathbb{U}_r , \mathbb{U}_g , \mathbb{U}_b , to the holes of the pants. Essentially, we arrive at a commutative diagram:

$$\begin{array}{ccc} \mathcal{P}(R_3) & \xrightarrow{\text{inclusion}} & \mathbb{C}P^1 \\ & \searrow p(y) & \downarrow \tilde{p} \text{ is branched covering.} \\ & & \mathbb{C}P^1 \end{array} \quad (4.3)$$

Applying the Riemann–Hurwitz formula for the holomorphic mapping \tilde{p} with four ramification points (three of them are in the artificially glued discs and the fourth is inside the pants) we immediately get:

$$d_r + d_g + d_b = 2N, \quad N := \deg \tilde{p}. \tag{4.4}$$

4.1.3. Intersection of Circles.

Lemma 4.1. *The circle C does not intersect the two other circles $\varepsilon^{\pm 1}\hat{\mathbb{R}}$. Therefore the spectral parameter $1 < \lambda < 2$ when the projective structure $p(y)$ branch point is inside the pants.*

Proof. : We know that the point 0 lies in the intersection of two of our circles: $\varepsilon\hat{\mathbb{R}}$ and $\varepsilon^2\hat{\mathbb{R}}$. The total number $\#\{\tilde{p}^{-1}(0)\}$ of the pre-images of this point (counting the multiplicities) is N and cannot be less than $d_b + d_g$ – the number of pre-images on the blue and green boundary components of the pants. Comparing this to (4.4) we get $d_r \geq N$ which is only possible when

$$d_r = d_g + d_b = N. \tag{4.5}$$

Assuming that the circle C intersects any of the circles $\varepsilon^{\pm 1}\hat{\mathbb{R}}$ we repeat the above argument for the intersection point and arrive at the conclusion $d_b = d_r + d_g = N$ or $d_g = d_r + d_b = N$ which is incompatible with the already established equation (4.5). \square

Remark 4.2. In section 3.4.3 we promised to show that any meromorphic function p mapping the boundaries of the pants to the circles (3.29) has a *critical point*. Indeed, the inequalities $d_b + d_g \leq N$ and $d_r \leq N$ remain true whatever the branching of the structure p is, while (4.4) originating from the Riemann–Hurwitz formula takes the form $d_b + d_g + d_r = 2N + 1$ for the *unbranched* structure which leads to a contradiction.

4.1.4. Image of the Pants. Let us investigate where the artificially glued discs are mapped to. Suppose for instance that the disc \mathbb{U}_r is mapped to the exterior of the circle C . The point 0 will be covered then at least $d_r + d_g + d_b = 2N$ times which is impossible. The discs \mathbb{U}_g and \mathbb{U}_b are mapped to the left of the lines $\varepsilon\mathbb{R}$ and $\varepsilon^2\mathbb{R}$ respectively, otherwise points from the interior of the circle C will be covered more than N times. The image of the pair of pants $\mathcal{P}(R_3)$ is shown on the left of the Fig. 6.

We use the ambiguity in the construction of the glueing of the disks to the pants and require that the critical values of \tilde{p} in the discs $\mathbb{U}_g, \mathbb{U}_b$ coincide. Now the branched covering \tilde{p} has only three different branch points shown as \bullet, \circ and $*$ on the Fig. 6a). The branching type at those three points for $d_g = 2, d_b = 3, d = N = 5$ is shown on the Fig. 6b). The coverings with three branch points are called *Belyi maps* and are described by certain graphs known as Grothendieck’s “*Dessins d’Enfants*”. In our case the *dessin* is the lifting of the segment connecting white and black branch points: $\Gamma := \tilde{p}^{-1}[\bullet, \circ]$.

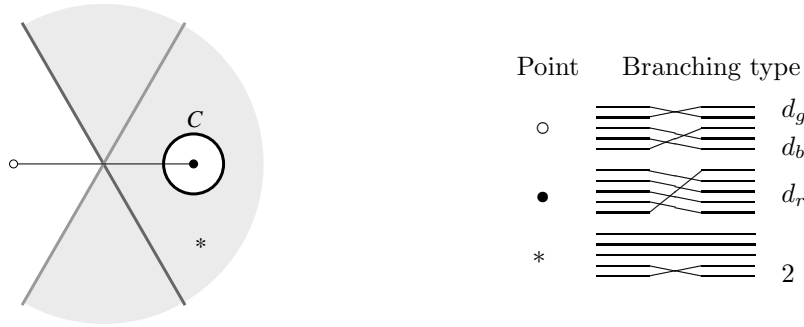


FIGURE 6. (a) Shaded area is the image of pants (b) Branching type of the branch points

4.1.5. Combinatorial Analysis of the Dessins. There is exactly one critical point of \tilde{p} over the branch point $*$. Hence, the complement to the graph Γ on the upper sphere of the diagram (4.3) contains exactly one cell mapped $2 - 1$ to the lower sphere. The rest of the components of the complement are mapped $1 - 1$. Two types of cells are shown in figures 7 a) and b), the lifting of the red circle is not shown to simplify the pictures. The branch point $*$ should lie in the intersection of the two annuli α and $\bar{\alpha}$, otherwise the discs $\mathbb{U}_g, \mathbb{U}_b$ glued to different boundary components of our pants will intersect: the hypothetical case when the branch point of $p(y)$ belongs to one annulus but does not belong to the other is shown in Fig. 7 c).

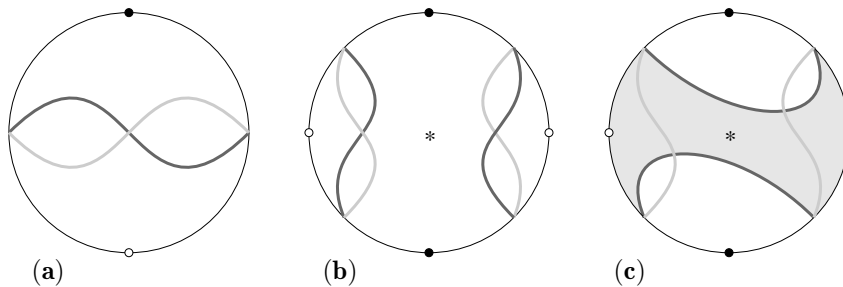


FIGURE 7. (a) Simple cell (b) Double cover (c) Impossible double cover

The cells from Fig. 7 a), b) may be assembled in a unique way shown in Fig. 8. The pants are colored in white, three artificially sewed discs are shaded. Essentially this picture shows us how to sew together the patches bounded by our three circles $C, \varepsilon^{\pm 1}\hat{\mathbb{R}}$ to get the pants conformally equivalent to $\mathcal{P}(R_3)$. As a result of the surgery procedure we obtain the pants $\mathcal{P}_1(\lambda, h_1, h_2 | d_g - 1, d_b - 1)$.

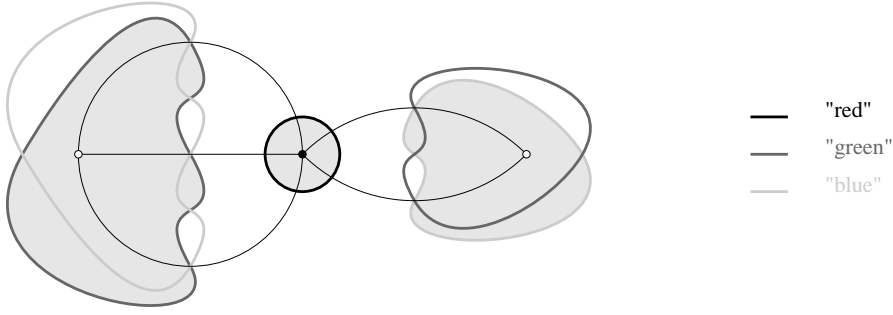


FIGURE 8. Dessin for $d_g = 3, d_b = 2$; the pre-image of the branch point $*$ is at the infinity

4.2. Simple branch points on the boundary of the pants

Our strategy remains the same: to fill in the holes in the pants and to convert $p(y)$ into a branched covering with a simple type of branching.

4.2.1. Construction 2. Let again $p(y)$ be a holomorphic mapping of a bounded Riemann surface \mathcal{M} to the sphere with the selected boundary component $(\partial\mathcal{M})_*$ being mapped to the boundary of the unit disc \mathbb{U} . Now the mapping $p(y)$ has two simple critical points on the selected boundary component (the case of coinciding critical values is not excluded). Those two points divide the oval $(\partial\mathcal{M})_*$ into two segments: $(\partial\mathcal{M})_*^+$ and $(\partial\mathcal{M})_*^-$. Let the increment of $\arg p(y)$ on the segment $(\partial\mathcal{M})_*^+$ be $2\pi d^+ - \phi$, $0 < \phi \leq 2\pi$, and the decrement on the segment $(\partial\mathcal{M})_*^-$ be $2\pi d^- - \phi$, the point y moves around the selected oval in the positive direction and d^\pm are positive integers. We are going to fill in the hole in the Riemann surface \mathcal{M} with two copies of the unitary disc (4.1): \mathbb{U}^+ and \mathbb{U}^- .

We define the mapping from the disjoint union $\mathcal{M} \cup \mathbb{U}^+ \cup \mathbb{U}^-$ to the sphere:

$$\tilde{p}(y) := \begin{cases} p(y), & y \in \mathcal{M}, \\ L^-(y^{d^-}), & y \in \mathbb{U}^-, \\ L^+(y^{-d^+}), & y \in \mathbb{U}^+, \end{cases} \quad (4.6)$$

where $L^\pm(\cdot)$ are the (at the moment arbitrary) linear fractional mappings keeping the unitary disc (4.1) invariant. The choice of $L^\pm(\cdot)$ will be specified later to simplify the combinatorial analysis.

Identifying the points y with the same value of $\tilde{p}(y)$ we glue the segments $(\partial\mathcal{M}^*)^\pm$ of the selected boundary oval of \mathcal{M} to the portions of the boundaries of the discs \mathbb{U}^\pm respectively. The remaining parts of the boundaries of \mathbb{U}^\pm are glued to each other as shown in Fig. 10a).

4.2.2. Branched Covering of a Sphere. At the moment we do not know which of the three boundary ovals of the pants $\mathcal{P}(R_3)$ contains the critical points of $p(y)$. Therefore we introduce the 'nicknames' $\{1, 2, 3\}$ for the set of colors $\{r, g, b\}$ so

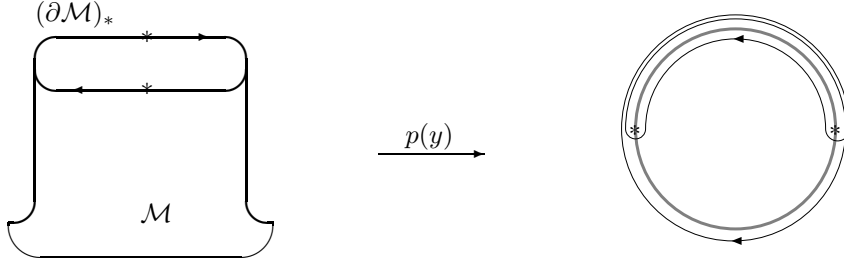


FIGURE 9. Mapping of the boundary component $(\partial\mathcal{M})_*$ with two simple branch points $*$ on it and winding indices $d^+ = 1, d^- = 2$.

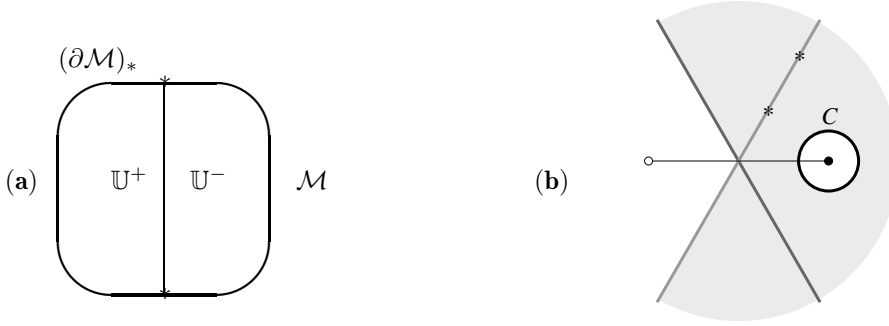


FIGURE 10. (a) Filling in the hole bounded by $(\partial\mathcal{M})_*$ (b) The shaded area is the image of $\mathcal{P}(R_3)$.

that the critical points will be on the oval number 3. The usage of *construction 2* from section 4.2.1 allows us to glue two discs \mathbb{U}_3^\pm to the latter boundary. The usage of *construction 1* from section 4.1.1 fills in the remaining two holes with two discs \mathbb{U}_1 and \mathbb{U}_2 . Positive integers arising in those constructions are denoted by d_3^\pm, d_1, d_2 respectively.

Again, we split the mapping $p(y)$ from the pants to the sphere as in the diagram (4.3): $p = \tilde{p} \circ \text{inclusion}$ with the branched covering \tilde{p} . The latter mapping has six critical points: two simple ones inherited from the pants and four at the centers of the artificially glued discs and multiplicities $d_3^\pm - 1, d_1 - 1, d_2 - 1$ respectively. The Riemann–Hurwitz formula for this covering gives

$$d_1 + d_2 + d_3^+ + d_3^- = 2N, \quad N := \deg \tilde{p}. \quad (4.7)$$

Lemma 4.3. *The images of the ovals with numbers 1 and 2 do not intersect.*

Proof. Suppose the opposite is true and a point Pt lies in the intersection of the images of the first two ovals. Then $N \geq \#\tilde{p}^{-1}(Pt) \geq d_1 + d_2$. On the image of the third oval there is a point (e.g. in the right side of Fig. 9 this is a point i) with $d_3^+ + d_3^- \leq N$ pre-images. Comparing the last two inequalities to (4.7) we get the

equalities

$$d_1 + d_2 = d_3^+ + d_3^- = N$$

and Pt is covered at least $d_1 + d_2 + \min(d_3^+, d_3^-) > N$ times. \square

Corollary 4.4. *Two circles $\varepsilon^{\pm 1}\hat{\mathbb{R}}$ intersect, therefore the critical points of $p(y)$ lie either on the blue or on the green boundary of pants. Moreover, the circle C – the image of the red boundary oval – does not intersect the two mentioned circles which may only happen when $\mu \in (\frac{1}{2}, 1)$, or equivalently $\lambda \in (1, 2)$.*

Convention: We assume that both critical points of p lie on the blue oval. The remaining case when they belong to the green oval is absolutely analogous to the case we consider. Now the notations $\mathbb{U}_b^\pm, \mathbb{U}_r, \mathbb{U}_g, d_b^\pm, d_r, d_g$ have the obvious meaning.

4.2.3. The Image of the Pants. Let us show that the the image of the pants remains the same as in section 4.1.4.

Lemma 4.5. *The image $p(\mathcal{P}(R_3))$ of the pants lies in the intersection of annuli α and $\bar{\alpha}$ – see Fig. 10b)*

Proof. We refer to the four sectors: $\mathbb{C} \setminus \varepsilon^{\pm 1}\mathbb{R}$ as to 'top', 'down', 'left' and 'right'. It is a matter of notation to say that the disc \mathbb{U}_b^+ is mapped to the 'top' and 'left' sectors while the disc \mathbb{U}_b^- is mapped to the 'down' and 'right' sectors.

The disc \mathbb{U}_g covers either the 'top' or the 'left' sector and both are covered by the disc \mathbb{U}_b^+ . Therefore, $d_g + d_b^+ \leq N$. In a similar way we get $d_r + d_b^- \leq N$. The obtained inequalities and the Riemann–Hurwitz formula (4.7) – which in our notations becomes $d_r + d_g + d_b^+ + d_b^- = 2N$ – give us

$$d_r + d_b^- = d_g + d_b^+ = N.$$

If the disc \mathbb{U}_r is mapped to the exterior of the circle C , then either 'left' or 'top' sector is covered $d_r + d_g + d_b^+ > N$ times. If the disc \mathbb{U}_g is mapped to the right of the line $\varepsilon\mathbb{R}$, then the interior of the circle C is covered $d_r + d_g + d_b^- > N$ times.

We see that the 'left' sector and the interior of the circle C are covered by the artificially inserted discs only. \square

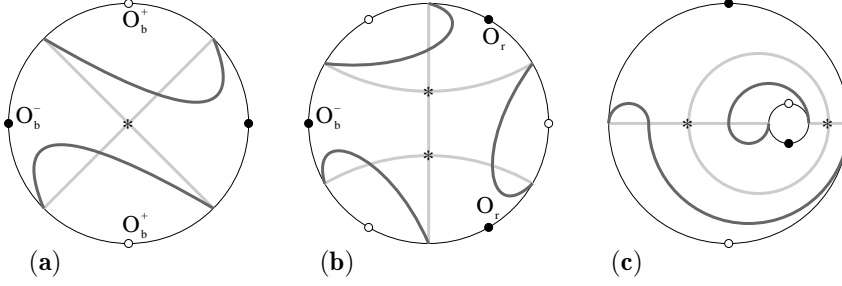
Corollary 4.6. *Both critical values of $p(y)$ lie on the ray $-\varepsilon^2(0, \infty)$.*

Corollary 4.7. *The integer d_b^- is equal to 1, since the point 0 is covered at least $d_g + d_b^+ + d_b^- - 1 \leq N$ times.*

Let us recall that the constructions of attaching discs to the pants allow us to move branch point (= the critical value of $\tilde{p}(y)$ in the inserted disc) within the appropriate circle. In particular, the critical values of $\tilde{p}(y)$ in the discs $\mathbb{U}_g, \mathbb{U}_b^+$ may be placed to the same point in the 'left' sector, say to $p = -1$ (point \circ in Fig. 10b) while the critical values in the discs $\mathbb{U}_r, \mathbb{U}_b^-$ may be placed to the same point inside C , say to $p = 1$ (point \bullet in Fig. 10b). Now we lift the segment $[\circ, \bullet]$

TABLE 2. Flat surfaces F covering the disc with the branching number $B \leq 2$

number of sheets	B	surface F	picture
1	0	disc	Fig. 7(a)
2	1	disc	Fig. 11(a)
3	2	disc	Fig. 11(b)
2	2	annulus	Fig. 11(c)

FIGURE 11. Flat surfaces F covering the disc with the branching numbers $B = 1, 2$.

connecting the branch points to the upper sphere of the diagram (4.3) and analyze the arising graph $\Gamma := \tilde{p}^{-1}([\circ, \bullet])$.

4.2.4. Combinatorial Analysis of the Graph. The restriction of \tilde{p} to every component F of the compliment $\hat{\mathbb{C}} \setminus \Gamma$ to the graph is naturally continued to the branched coverings over the disc² $\text{Closure}(\hat{\mathbb{C}} \setminus [\circ, \bullet])$. We can list all flat surfaces F covering a disc with the branching number $B \leq 2$. To this end we use the Riemann–Hurwitz formula for the branched coverings of the bordered surfaces:

$$2 + B = \#\{\partial F\} + \deg \tilde{p}|_F$$

which relates B – the total branching number of \tilde{p} in the selected flat surface F covering a disc; $\#\{\partial F\}$ – the number of its boundary components and $\deg \tilde{p}|_F$ – the degree of the restriction of the covering \tilde{p} to the component F . Taking into account that $\#\{\partial F\} \leq \deg \tilde{p}|_F$ we obtain the list shown in Tab. 2.

The combinatorics of the green and blue circles lifted to the listed covering surfaces F is shown in the Fig. 7a) and Fig.11a-c). Let us denote the centers of the four artificially glued discs $\mathbb{U}_r, \mathbb{U}_g, \mathbb{U}_b^+, \mathbb{U}_b^-$ as respectively O_r (black vertex of graph Γ with valency d_r), O_g, O_b^+ (white vertexes with valencies d_g, d_b^+) and O_b^- (dangling black vertex). Their mutual positions in the graph Γ are subject to the following restriction:

²*Closure* here has the same meaning as in the formula (2.1)



FIGURE 12. If O_g and O_b^- were neighbors, the discs \mathbb{U}_b^- and \mathbb{U}_g would intersect.

Lemma 4.8. *The vertices O_g and O_b^- are not neighbors in Γ .*

Proof. The disjoint discs \mathbb{U}_b^- and \mathbb{U}_g of the upper sphere in the diagram (4.3) would intersect otherwise – see Fig. 12. \square

Corollary 4.9. *The vertices on the border of the triply covering disc F – see Fig. 11b) – appear in the following order: $O_g, O_r, O_b^+, O_b^-, O_b^+, O_r$.*

They may be uniquely ascribed to the vertices in the picture after the observation: *the blue line divides the vicinity of any critical point $*$ into four quadrants, two of which belong to the pair of pants, one belongs to the disc \mathbb{U}_b^- , and the rest is contained in the disc \mathbb{U}_b^+ .*

Corollary 4.10. *The complement to the graph Γ cannot contain two doubly covering discs F .*

Indeed, the point O_b^- lies on the boundary of one of those discs. Both neighboring vertices on the boundary of the disc F should be O_b^+ according to the lemma. But this contradicts the above *observation*: two quadrants of this covering disc belong to \mathbb{U}_b^+ – see Fig. 11a).

4.2.5. Assembly Scheme. We see that there remain only two possibilities for the complement to the graph Γ . It consists either of **(a)** one disc mapped 3-1 and $N - 3$ simple cells mapped 1-1 or **(b)** an annulus mapped 2-1 and $N - 2$ simple discs mapped 1-1. The graphs Γ with complement containing no simple cells are shown in Fig. 13. They correspond to the pants $\mathcal{P}_2(\dots|0, 1)$ **(a)** and $\mathcal{P}_2(\dots|0, 0)$ **(b)**. The graphs with simple cells in the complement are obtained from those two basic pictures as a result of the surgery. We cut the graph along the edge $O_r O_g$ and insert $d_g - 1$ simple discs in the slot as in Fig. 8. The graph on the left side of the Fig. 13 admits another surgery: we cut the graph along the edge $O_r O_b^+$ and sew in $d_b^+ - 2$ patches shown in Fig. 7a) in the slot. The arising graph corresponds to the pair of pants $\mathcal{P}_2(\dots, d_g - 1, d_b^+ - 1)$.

4.3. Remaining cases

If the branch points of the projective structure $p := p^+$ belong to the green oval of the pants we arrive at the pair of pants \mathcal{P}_s of fashion $s = 3$. Finally, when the branch points merge the limit variant of construction 2 may be applied for the analysis and we arrive at the pants of intermediate types $s = 12, 13$.

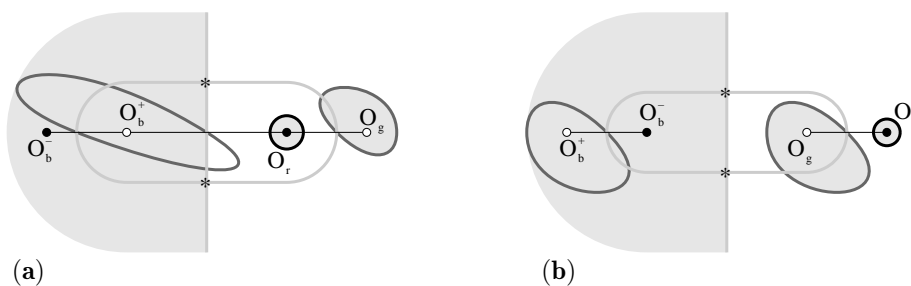


FIGURE 13. Graph Γ for the basic mappings with $d_g = 1$, $d_b^+ = d_r = 2$, $N = 3$ (a) and $d_g = d_b^+ = d_r = 1$, $N = 2$ (b). Artificially inserted discs are shaded.

5. Conclusion

A similar analysis based on the geometry and combinatorics may be applied to obtain the representations of the solutions of the PS-3 integral equation in all the omitted cases. Much of the techniques used may be helpful for the study of other integral equations with low degree rational kernels.

References

- [1] Agranovich M.S., Katzenelenbaum B.Z., Sivov A.N., Voitovich N.N.: *Generalized Method of Eigenoscillations in Diffraction Theory*. Wiley-VCH, Berlin (1999)
- [2] Bogatyrev A.B.: *The discrete spectrum of the problem with a pair of Poincare-Steklov operators*. Doklady RAS, **358**:3, 40-42 (1998)
- [3] Bogatyrev A.B.: *A geometric method for solving a series of integral PS equations*. Math. Notes, **63**:3, 302-310 (1998)
- [4] Poincare H.: *Analyse des travaux scientifiques de Henri Poincare*. Acta Math. **38**, 3-135 (1921)
- [5] Gunning R.C.: *Special coordinate coverings of Riemann surfaces*. Math. Annalen, **170**, 67-86 (1967)
- [6] Mandelbaum R.: *Branched structures and affine and projective bundles on Riemann surfaces*. Trans. AMS, **183**, 37-58 (1973)
- [7] Hejhal D.A.: *Monodromy groups and linearly polymorphic functions*. Acta Math., **135**, 1-55 (1975)
- [8] Tyurin A.N.: *On the periods of quadratic differentials*. Russian Math. Surveys, **33**:6, 149-195 (1978)
- [9] Gallo D., Kapovich M., Marden A.: *The monodromy groups of Schwarzian equations on closed Riemann surfaces*// Ann. of Math. (2) **151**:2, 625-704 (2000); also arXiv, math.CV/9511213
- [10] Bogatyrev A.B.: *Poincare-Steklov integral equations and the Riemann monodromy problem*. Funct. Anal. Appl. **34**:2, 9-22 (2000)

- [11] Bogatyrev A.B.: *PS-3 integral equations and projective structures on Riemann surfaces*. Sbornik: Math., **192**:4, 479-514 (2001)

Andrei Bogatyrev
INM RAS, ul. Gubkina, 8
Moscow GSP-1,
119991 Russia
e-mail: gourmet@inm.ras.ru